Effect of Tip Clearance and Rotor-Stator Axial Gap onAxial CompressorPerformance

A Thesis Submitted

In partial fulfillment for the reward of the degree of

Master of technology

In Mechanical Engineering

Submitted By

Ayush Tyagi

(2K19/THE/04)

Under the Guidance

of

Dr. Anil Kumar

Associate Professor

Department of Mechanical, Production & Industrial and Automobile Engineering

Delhi Technological University

Bawana Road, Delhi-110042

CANDIDATE'S DECLARATION

I, here by certify that the work which is being presented in thesis entitled "EFFECT OF TIP CLEARANCE AND ROTOR-STATOR AXIAL GAP ON THE PERFORMANCE OF AXIAL COMPRESSOR" being submitted by me is an authentic record of my own work carried out under the supervision of Associate Professor Dr.Anil Kumar, Department of Mechanical Engineering, Delhi Technological University Delhi.

The matter presented in this thesis has not been submitted in any other University/Institute for the award of M.Tech Degree.

Ayush Tyagi

(2K19/THE/04)

CERTIFICATE

I, hereby rectify that the work which is being presented in this thesis entitled "EFFECT OF TIP CLEARANCE AND ROTOR-STATOR AXIAL GAP ON THE PERFORMANCE OF AXIAL COMPRESSOR" in the partial fulfillment of requirement for the reward of degree of Masters of Technology in Thermal Engineering submitted in the Department of Mechanical Engineering, Delhi Technological University Delhi is an authentic record of my own work carried out during a period from July2020 to June 2021, under the supervision of Associate Professor Dr. Anil Kumar, Department of Mechanical Engineering, Delhi Technological University Delhi.

The matter presented in this thesis has not been submitted in any other University/Institute for the award of M.Tech. Degree.

Dr. Anil Kumar
Supervisor
Department of Mechanical Engineering
Delhi Technological University, Delhi

ACKNOWLEDGEMENT

First and foremost, praise and thanks goes to my God for the blessing that has bestowed upon me in all my endeavors.

I am profoundly thankful of the inspiration, direction, titillation and patience of Dr. Anil Kumar, Associate Professor, my advisor and guide. I appreciate his wide range of experience and attention to detail, as well as his consistent support over the years. It should not be mentioned that a large part of this study is a consequence of collaborative collaboration, without which it would not have been possible to complete the work.

I sincerely thank Dr. Anil Kumar for his guidance and relentless support overthe year. I am thankful for his worthy suggestions and timelycooperation during his work on the project.

I would like to extend my gratitude to Prof. S. K. Garg, Head, Mechanical Engineering Department for providing this opportunity to carry out this present work.

I would like to thank my family members in this occasion for their moral support and motivation to complete this project in due course.

Ayush Tyagi

(2K19/THE/04)

ABSTRACT

The goal of this thesis is to expand on current understanding about tip clearance and rotor-stator axial hole on engine performance, with a focus on faster-equipment components (i.e. enthusiasts or compressors). Various high-fidelity three-dimensional Computational Fluid Dynamics (CFD) models have been developed using a transonic compressor degree (i.e. NASA stage 37). The current research focuses on the effect of rotor tip clearance on the degree of a transonic axial compressor. Because of the relative motion between the rotor and stator blades, the float subject on this equipment is very unstable.Furthermore, the device is complicated by a variety of technological consequences such as tip clearances, blade complexity, and axial distance variations between the stator and rotor. As a result, one of the most challenging tasks a CFD professional can accomplish is to investigate a complicated, strongly 3-dimensional flow discipline inside a compressor. The NASA 37 transonic axial compressor degree with a rotor tip clearance of 0.5mm is investigated utilising numerical simulations using the ANSYS CFX software package. All simulations for the first stage, Rotor–Stator, were run. The experimental investigation and the standard performance parameters acquired from modelling of tip clearance were found to be in good agreement.

Table of Contents

Title
Page No

LIST OF FIGURES

ABBREVIATIONS

3D	Three Dimensional
CAD	Computer Aided Design
CFD	Computational Fluid Dynamics
NASA	National Aeronautics and Space Administration
RANS	Reynolds Averaged Navier-Stokes
URANS	Unsteady Reynolds Averaged Navier-Stokes
RPM	Revolutions per Minute
k	Turbulent kinetic energy (J)
TC	Tip clearance gap in mm
ρ	Density (kg/m^3)
η	Efficiency (%)
S1	Stator 1
R1	Rotor 1
M	Mach number
m	Mass flow rate (kg/s)
PR	Pressure Ratio
TR	Temperature ratio
SST	Shear Stress Transport

CHAPTER 1

INTRODUCTION

1.1 BACKGROUND

An air compressor is a device which is used to enhance pressure of air on the expanses of its volume. Compressor are similar to pump but compressor are used to increase the pressure of air on the other hand pump is used to increase to pressure of water. Compressor are mainly multi staged because to develop a very high pressure and also by using multi stage the work done required decrease along with-it uniform torque is obtained.

RECIPROCATING COMPRESSOR

Reciprocating Compressor are used to supply air at very large pressure and when where less amount of flow rate is required. In reciprocating compressor, the supply of air is intermittent as the supply air is available only in one stroke so these compressors are mainly multi staged. The speed of these compressor ais also low so they can not be coupled with turbine.

Multi stage has many advantages over single stage like it has high volumetric efficiency, reduced driving power. They are generally used in Refrigeration system

ROTARY COMPRESSOR

Rotary compressor are compressor in which kinetic energy is supplied to water by an rotating element and then this kinetic energy is used to increase the pressure in a device called diffuser. Rotary compressor are used to supply continuous compressed air. Rotary compressor are consisted of an rotor and casing in place of piston cylinder arrangement. Rotary compressor work on low head and high discharge with high efficiency and due to low starting torque, they can be directly coupled with prime mover. Rotary compressor works on large range of mass and are suitable for low and medium pressure ratio.

Rotary compressor are mainly of two types:

1. Centrifugal Compressor
2. Axial Compressor

CENTRIFUGAL COMPRESSOR

Centrifugal compressor is not used in gas turbine because of low speed and large frontal area but they also have some advantages like they occupy smaller length when compared to axial flow compressor and also the quality of fluid does not affect the performance of centrifugal compressor whereas in axial compressor the performance depends largely on quality of fluid. Also, they work on wider range of mass flow rate.

The pressure ratio that can be obtained in a single stage centrifugal compressor is 5:1. The main parts of centrifugal are:

Inlet Casing

1. Impeller
2. Diffuser
3. Outer Casing

In centrifugal compressor there are some losses also due to flow of fluid in compressor. These losses are Frictional losses, Incidence Losses and pressure losses. These losses can be decreased by lowering fluid flow velocity and expanding the diameter of conduit through which the fluid flows.

AXIAL COMPRESSOR

Axial compressor are mainly used in gas turbine power plant and especially in aircraft application. Because of small frontal area they are used in aircraft application and because of high speed they can be directly coupled to the turbine.

In axial compressor there are number of stages each stage consisting of Fixed Blade and Moving Blade. In axial compressor fluid enters compressor in axial direction. Mass flow rate remains constant in the stages of compressor but in higher stage as pressure increase the density decrease and to maintain mass flow rate constant the area has to be decreased so as to maintain constant velocity throughout the compressor.

In centrifugal compressor the losses are of mainly two types :

1. Profile Loss
2. Tip Clearance Loss

In the context of this project which is mainly applicable to the field of gas turbine propulsion, it would be apt to give a brief overview of the gas turbine engine and its application in aircraft propulsion.

The Gas Turbine Engine is the primary means of propulsion for ships, submarines etc. in general and aircrafts in particular. The Gas Turbine Engine as applicable to aircraft propulsion consists of the following parts: -

1. Inlet
2. Compressor
3. Combustion chamber
4. Turbine

5. Propelling nozzle

The gas generator is made up of combustion chamber, compressorand turbine, and is entirely responsible for producing high temperature and high pressure air for propulsion. The compressor and turbine are usually in stages and are attached the same shaft i.e. the turbine stages run the compressor stages.The turbine accomplishes this by taking work from the combustion chamber's high-pressure, high-temperature air and expanding it via the stator and rotor blades. Thrust is produced when the expanded air from the turbine is further expanded in the pushing nozzle.

A multi-stage axial compressor can be used in a variety of industries. It is a significant gas turbine engine used in steam power plants and aviation. Axial flow compressors are typically found in high-volume systems like turbine engines. The overall efficacy of this sort of equipment is mostly determined by the axial compressor's performance. As a result, employing CFD methods to investigate the efficiency of compressor design is critical. However, because of the impact on machine efficiency, operational range, and stability, it is critical to understand the features of the flow field.

1.2 INVESTIGATION

The goal of this study is to look at tip clearance effect in a transonic axial compressor stage with different rotor tip clearances and rotor solidities. The NASA37 compressor's rotor tip clearance component is the subject of numerical investigations.

In this study ,the tip clearance is varied from design point of 0.36 mm to 0.5 mm and the results are compared to know its effect.

1.3OBJECTIVE

The goal of this research is to add to what we already know about the effects of clearance and axial gap on rotor stator engine performance by focusing on turbomachine components. A study of how the tip of the rotor blade and the axial gap in the rotor and

stator impact the performance of an axial compressor is done using software for computing the RANS equation.

CHAPTER 2

LITERATURE REVIEW

2.1 SURVEY

Subbaramu et al. [13]In this research was done on effect of secondary flow interaction and tip leakage on certain parameters which include stability and operation of a transonic axial compressor stage, and it was discovered that stall margin is greater at low rotor solidity (32 blades) and less at 36 blades. The change in tip leakage mass flow rate at varying rotor solidities is responsible for this activity.

Tang et al. [20]In compressor with an increase in tip clearance the similar loss behaviour is obtained and the best clearance calculated is 6 μm for their specific design.

Storer and Cumpsty [15]It was observed that tip leakage method is largely useless, and that leakage flow can have an impact on local pressure field. The size of leak's tip is always proportional to the aerodynamic loading of the pages and the tip gap.

Suder et al. [16] have discussed shock/leakage vortex leaks in the design of the wall closure at the end. According to the findings of shock interaction at a given speed, radial influence of tip clearance flow extends to 20 times actual tip clearance height. In the absence of shock, radial extent at half speed is only 5 times tip clearance height.

Lakshminarayana et al. [5] show that leakage jet does not eliminate the vortex as found in cascade studies. The high-velocity leakage jet that emerges from the tip gap mixes with the mainstream, resulting in significant shearing and flow separation.

Furukawa et al [3]The effect of restricted blade loading on the deterioration of tip leaking vortex at low speed axial compressor rotor has been explored. The leak vortex degeneration within the rotor happens at less flow rate than in high pressure operational state, according to the simulation.It was observed that degeneration of the leak vortex has a important role in in the aspect of rotor performance in conditions close to the stall. As the flow rate decreases from a working state of high pressure, the deteriorating region

grows rapidly in sloping, extended, and steep slopes, causing flow restriction, and the loss is greatly increased. The collapsing circuit's interaction with the metal suction creates a 3-D separation of earth's boundary layer, leading in a rapid reduction in total pressure over the Rotor.

Syed et al.[17]have investigated how the axial gap and tip clearance affect a multistage compressor's efficiency. Using the SpalartAllmaras model, Thermal Engineering modelled a well-known industrial compressor design and numerically analysed impact of tip clearance on performance of the axial compressor stage.

Sriram et al.[14] has performed Numerical Study of Pre-Diffuser Performance with Axial Flow Compressor in which he modelled the axial compressor .

Sakulkaew et al. [11]observed that for clearance gap in the range of 0.8% to 3.4% the efficiency decrease with increase in clearance. It is found that efficiency is less sensitive to gap more than 3.4%.

Gorrell et al. [9,10]"Exploring the influence of stator-rotor-stator spacing on axial compressor performance revealed that when metal lines are spaced tightly, losses in addition to mixing losses arise owing to shock creation of the recorded bow. This increased loss is linked to a rise in stator levels. The axial intervals between the ascending train and the lower transonic rotor have a substantial effect on the platform's performance, according to the data collected in this study." [17] It was observed that with reduction in axial space between the higher stator and the lower rotor shrank, the efficiency, pressure ratio and flow rate reduces.

2.2 SUMMARY OF LITERATURE

After analysing literature review we can conclude that there are mainly three impacts created by tip approval. They are:

(i) secondary flow due to pressure gradients
(ii) leakage flow through tip clearance due to pressure difference;
(iii) boundary scrapping effect due to blades moving relative to wall boundary layer

CHAPTER 3

METHODOLOGY

3.1 PROPOSED METHODOLOGY

First, designof investigated geometries (i.e. NASA Rotor 37 and stator 37), and their meshes were generated. In this study a commercial CFD software was used to conduct several test so that similarity can be obtained in the developed tool kit.With the help of literature review a number of methods were find out to imply boundary condition. A vast number of tests were undertaken to determine the BC implementation method's applicability. To perform a steady state Reynolds Averaged Navier Stokes a CFD capability is developed. With the help of this CFD software the key difference in terms of accuracy was analysed.

For a study to be helpful and accurate, a wide range of data must be collected. Throughout the investigation, data was collected in a systematic manner.

In order to reduce post-processing, a number of successful strategies were used and implemented. The data is efficiently handled using this way. This made it possible to process the data quickly. All of these procedures are completed in this study, and the tools from ANSYS Workbench 2020 R2 were used in the project.

• Mesh generation: ANSYS TurboGrid.

• CFD simulations: ANSYS CFX-Pre, and CFX-Solver.

• Post-analysis: ANSYS CFX-Post.

3.2 PRE REQUISITES

3.2.1 NAVIER – STOKES EQUATION

The Navier–Stokes equations, named after Claude-Louis Navier and George Gabriel Stokes. By applying Newton's second law to fluid motion, this balancing equations is obtained.

For compressible Newtonian fluid, it is given by: -

$$\rho\left(\frac{\partial \vec{u}}{\partial t} + \vec{u}.\nabla\vec{u}\right) = -\nabla p + \nabla.\left(\mu(\nabla\vec{u} + (\nabla\vec{u})^T) - \frac{2}{3}\mu(\nabla.\vec{u})I\right) + F$$

where,

$\vec{u}$ = fluid velocity vector

p = fluid pressure

I = Identity matrix

μ = fluid dynamic viscosity

ρ = fluid density

The terms in the above formula is: -

$\rho\left(\frac{\partial \vec{u}}{\partial t} + \vec{u}.\nabla\vec{u}\right)$ = Local and convective acceleration

$-\nabla p$ = Pressure gradient

$\nabla.\left(\mu(\nabla\vec{u} + (\nabla\vec{u})^T) - \frac{2}{3}\mu(\nabla.\vec{u})I\right)$ = Viscous forces

F = External forces applied to the fluid.

Above equation is always solved together with continuity equation: -

$$\frac{\partial \rho}{\partial t} + \nabla.(\rho\vec{u}) = 0$$

Mass conservation is given by the continuity equation, whereas momentum conservation is represented by the Navier– Stokes equation. It provides the solution for viscous fluid

that is for real fluid. These equations are used to find out pressure field when velocity field is known and also to find velocity profile for fluid flow.

3.2.2 REYNOLDS AVERAGED NAVIER STOKES EQUATIONS (RANS)

The RANS equations are time-averaged fluid flow equations. Reynolds decomposition is the concept behind the equations, which decomposes an instantaneous variable into its time-averaged and fluctuating components.RANS equations are as follows: -

$$\frac{\partial \rho}{\partial t}+\frac{\partial}{\partial x_i}(\rho u_i)=0 \quad \text{..... 1}$$

$$\frac{\partial}{\partial t}(\rho u_i)+\frac{\partial}{\partial x_j}\left(\rho u_i u_j\right)= -\frac{\partial p}{\partial x_i}+\frac{\partial}{\partial x_j}\left[\mu\left(\frac{\partial u_i}{\partial x_j}+\frac{\partial u_j}{\partial x_i}-\frac{2}{3}\delta_{ij}\frac{\partial u_l}{\partial x_l}\right)\right] + \frac{\partial}{\partial x_j}\left(-\rho\overline{u'_i u'_j}\right) \quad \text{..... 2}$$

$$\frac{\partial}{\partial t}(\rho E)+\nabla\cdot(\vec{v}\,(\rho E+p))=\nabla\cdot\left(k_{eff}\nabla T-\sum_j h_j\vec{J}_j+\left(\overline{\overline{\tau}}_{eff}\cdot\vec{v}\right)\right)+S_h \quad \text{..... 3}$$

Equation 1 represents continuity equation, Equation 2 represents momentum equation, and the Equation 3 represents energy equation.

The terms in equation 2 are similar to that of Navier Stokes equation but contains one additional term which is the fluctuating term (also called the Reynolds stress term). This is given by: -

$$\frac{\partial}{\partial x_j}\left(-\rho\overline{u'_i u'_j}\right)$$

This term adds additional unknowns to the equation which in turn require additional equations to solve them and give closure to the equation. These additional equations to attain closure are obtained by turbulence models, which will be explained in next section. The Ansys Fluent CFD software solves all fluid flow problems using the RANS and equations obtained from turbulence models.

3.3 TURBULENCE AND TURBULENCE MODELS

The fluid flow which is time dependent and have the chaotic behaviour is known as turbulence. It is commonly assumed that it is due to the fluid's overall inertia. Less inertia means flow is laminar.

Because the Navier-Stokes numerical solution is only accessible for laminar flow and not for turbulent flow, solving Navier Stokes equation for turbulent flow is extremely challenging. In turbulent flow there are two type of stress as compared to one in laminar flow and they are viscous stress and eddy stress. In laminar flow there is a phenomenon of Prandtl mixing length which is defined as the distance travelled by molecules in transverse direction to obtain the surrounding velocity. To solve turbulent flow by assuming it as laminar flow there is requirement of fine mesh so that result is accurate. But this result in a time -unsteady solution, which do not converge properly.

As a result, in actual computational fluid dynamics (CFD) applications, time-averaged equations such as RANS equations are used in conjunction with turbulence models for modelling turbulent flows. Some models include: -

1. Spalart–Allmaras (1 equation)
2. *k–ω* SST (2 equation)
3. *k–ε* (2 equation)
4. Transition SST (4 equation)
5. Transition k-kl-ω (3 equation)

The above turbulence and transition models add a variety of additional equations to bring closure to RANS equations.

In current project, three models were used, two transition models (k-kl-ω, transition SST) and one fully turbulent model (k-ω SST). Prior to varying boundary conditions, the turbulence model that best predicts the aerodynamic and thermal flow conditions was to be established. The flow was observed to change from laminar to turbulent and hence the transition models were observed to give best results, while the results of k-ω SST did not match with the experimental results and hence was discarded.

In case of film cooling k-ε model was considered. Description of each model is given below: -

3.3.1 STANDARD k-ε MODEL: -

This standard k-model uses model transport equations to calculate dissipation rate and turbulence kinetic energy (k). Findings for k are derived from precise equations of model transport equations, whereas the results for have some similarity to their mathematically exact equivalent.

The k-model solution takes the assumption that the flow is totally turbulent with minimum viscosity losses.

3.3.2 k-ω SST MODEL: -

Menter developed SST k- ω version to combine strong and accurate method of okay – ω model in near-wall vicinity with freestream independence of version in the a ways subject. To do this, okay- ε model is transformed into an okay - system. The SST ok-ω version is much like the same old okay-ω version, however includes following refinements: -

• Both original model k-ω and altered ok-ε are multiplied by a mixing feature, and both models are provided together. The mixing characteristic is set to one near wall, which activates normal k-ω version, and 0 away from floor, which activates altered k-ε version.

• The SST model carries a damped cross-diffusion by-product time period inside the ω equation.

These qualities make SST ok-model more accurate and trustworthy than normal k-ω model over a significantly larger f flows (such as negative stress gradient flows, airfoils, and transonic surprise waves).

3.3.3 TRANSITION k-kl-ω: -

This model is use to analyse boundary layer development and compute transition onset.

The transport equations for turbulent kinetic energy (k), laminar kinetic energy (kl), and inverse turbulent time scale are included in this three-equation eddy-viscosity model ().

3.4INVESTIGATED NASA GEOMETRIES

Accurate geometric data is safeguarded by strong intellectual property restrictions in the aerospace sector. NASA, on other hand, makes a range of experimental test data available in the public domain in the form of technical papers. For decades, NASA experimental records were utilised to confirm the CFD results, with the usage of the precise universal NASA geometry. A detailed description of the two rotors, as well as the stator geometry studied on this occasion, is provided. In addition, CFD results of other researchers are covered, showing the main waft-subject functions.

3.4.1NASA ROTOR 37

In 1970, Nasa created Rotor 37. It's a rotor for a transonic high-pressure compressor that's part of an eight-sage compressor. Reid and Moore put it to the test at NASA's Lewis Research Center. The following are the major features of this rotor. Many research have employed this rotor, and the approach known as waft discipline analysis has been proposed. A photograph of an actual check case, as well as the dimension stations of the rotor are proven.

Figure 1: Real Picture of NASA Rotor 37

Figure 2: Design Specifications of NASA 37 Transonic Axial Compressor Stage

S. No.	Parameter	Value
1	Stage total pressure ratio	2.05
2	Rotor total pressure ratio	2.11
3	Rotor Aspect Ratio	1.19
3	Corrected mass flow rate	20.11 kg/s
4	Rotational speed	17188.7 rpm
5	Stage isentropic efficiency	84 %
6	Rotor inlet relative Mach number	1.13 (hub) / 1.48 (tip)
7	Number of rotor / stator blades	36 / 46
8	Rotor tip diameter	252 mm
9	Rotor hub-tip ratio	0.7
11	Rotor tip clearance	0.36 mm
12	Rotor tip chord	56 mm

The Transonic axial stage which consists of a rotor and stator was used for analysis as shown below.

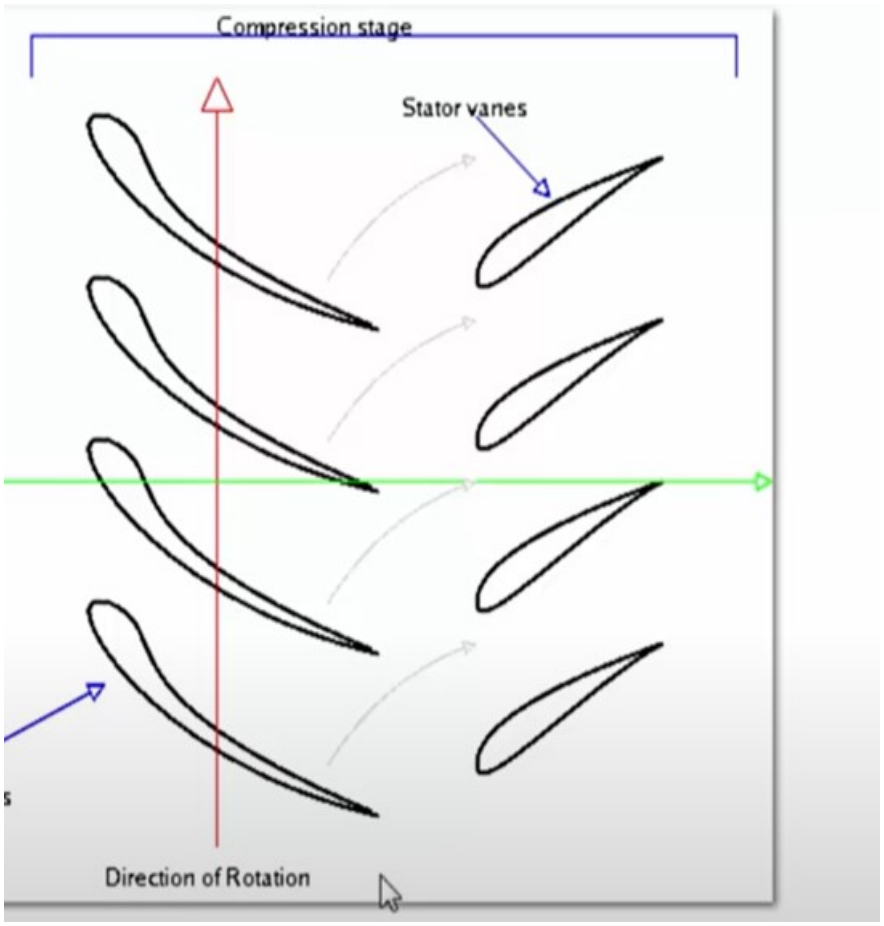

Figure 3: Axial compressor Stage

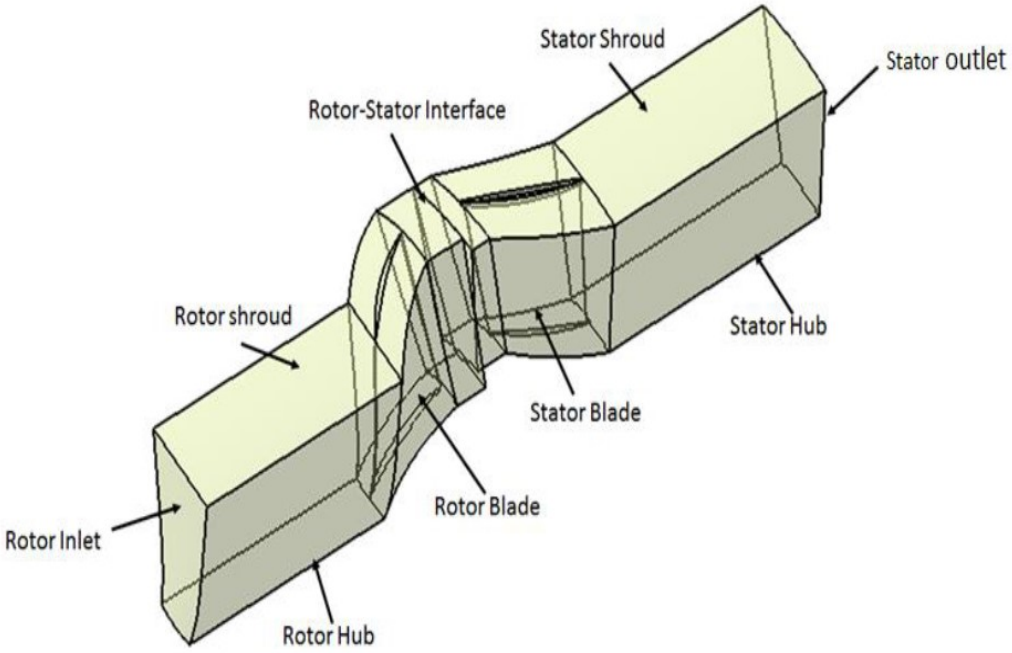

Figure 4: CAD model of NASA 37 stage periodic sector showing one rotor and one stator blade

The CAD model for only one rotor and one stator blade passage was created utilising profile coordinates of hub, shroud, and blade of rotor 37 and Stator 37 in Ansys Turbogrid due to rotational symmetry.

3.5GRID GENERATION

Ansys Turbogrid was used to create the mesh. It automatically creates mesh for turbomachinery setup, including orthogonality and mesh quality control options. A three-dimensional image of one of stage meshes is displayed. Skin-topology is made up of five blocks: The blade is surrounded by an O-mesh skin block. Upstream of the leading edge is an H-mesh intake block. The H-mesh outlet block is positioned downstream from the trailing edge. Above the blade portion is an H-mesh that serves as the up block.

Underneath the blade portion is an H-mesh that acts as a down block. To identify an optimal, mesh-independent solution that meets the y+ criterion, simulations were run using coarse, medium, and fine meshes.

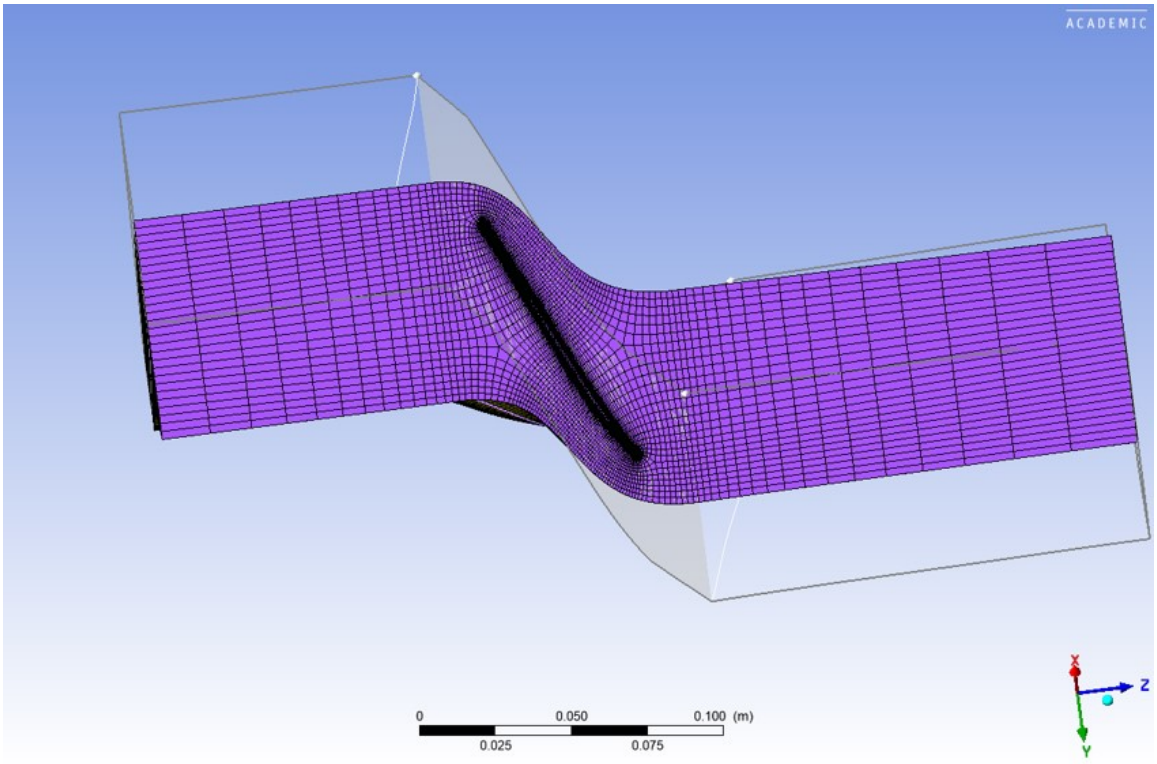

Figure 5: Mesh layer generated for Rotor 37

The mesh was generated using the Ansys Turbogrid .In the turbogrid there were options to choose from fine,coarse and medium mesh options.

All three different types of meshes were generated which consists of different no of cells.

1) Fine – 0.3 million cells.
2) Medium – 0.4 million cells.
3) Coarse – 0.6 million cells.

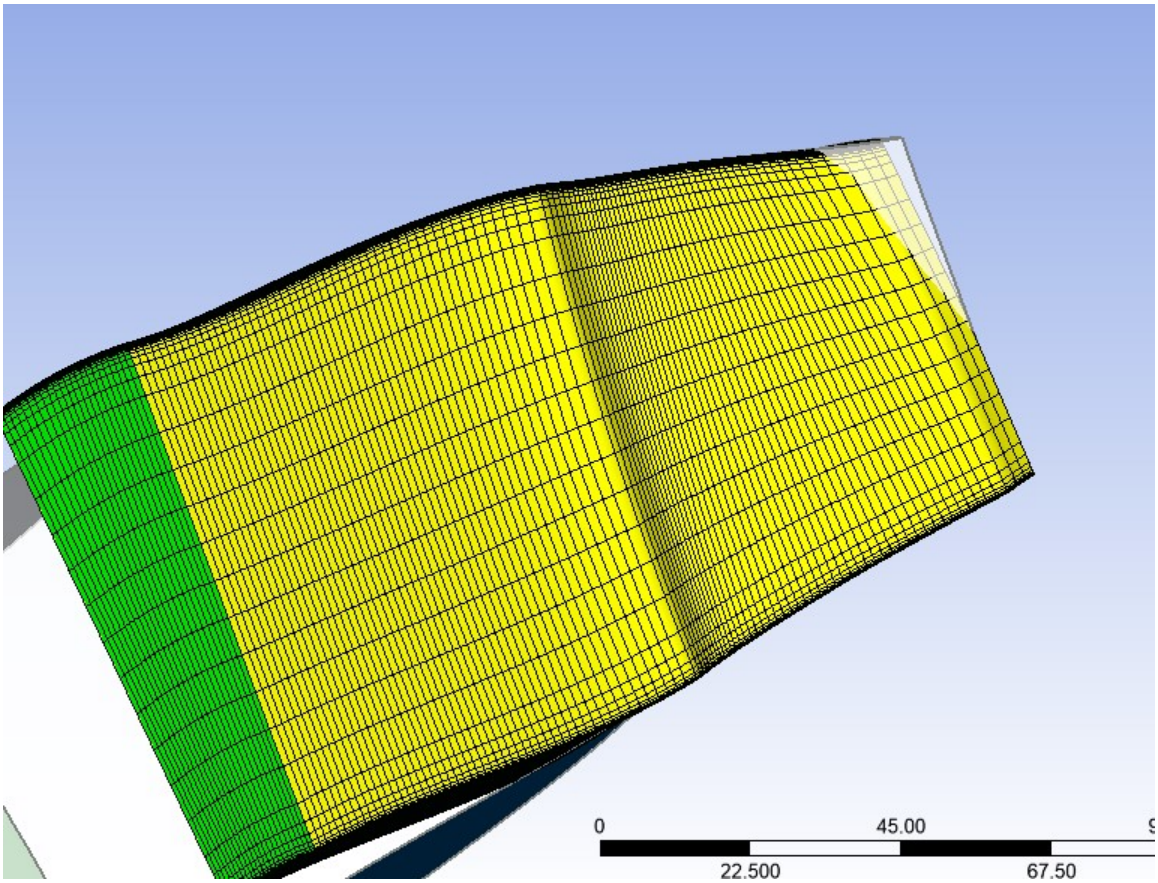

Figure 6: 3D Mesh Generated inTurbogrid

3.6 SOLVER SETTINGS

The ANSYS CFX software programme is used to solve governing float equations. RANS equations were solved using a three-dimensional, viscous, implicit segregated first order upwind technique based on constant state pressure. To simulate the turbulent flow, a generic ok-SST turbulence model with computerised wall characteristics is employed.The rotor domain on the hub wall's side is rotated around an rotation axis. Casing wall is rotated in the opposite direction as the rotor. All partitions are subjected to a no-slip drift condition. The entry glide circumstances included general stress, overall temperature, and drift angle, whereas the exit glide conditions included static pressure. The convergence step is complete for all simulations to a residual of 10-5. degree interface (blending plane method) is implemented between rotor and stator flow domains to transfer facts from rotor exit to stator inlet. Boundary situations used for stator and rotor domain are shown. Presure Inlet and static stress Outlet conditons is used for the analysis.

3.7 BOUNDARY CONDITIONS

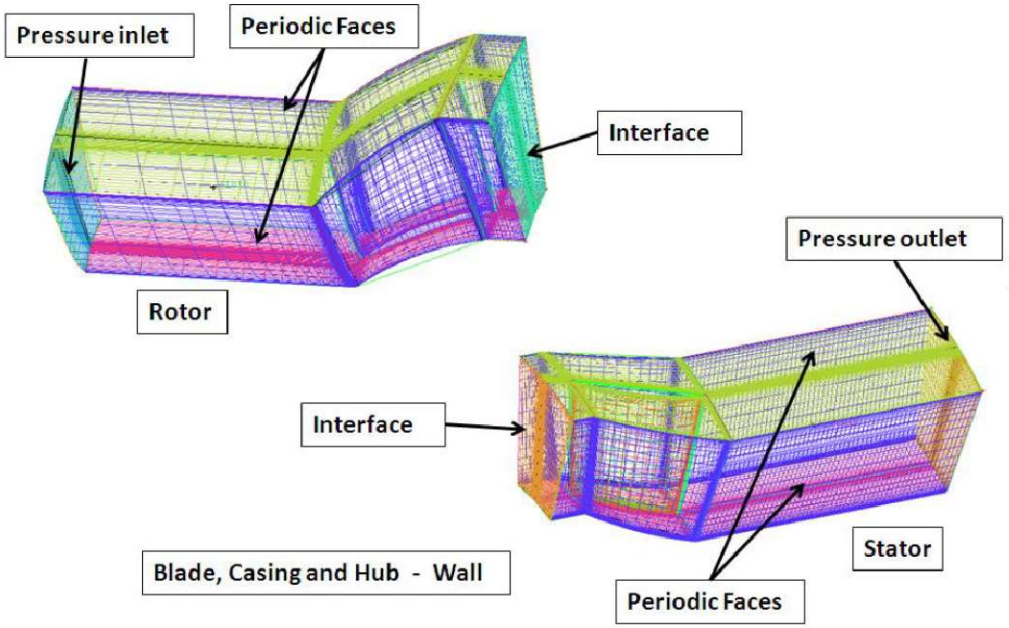

Figure 7:Boundary conditions for rotor and stator computational domains

Domain interfaces

Choice of domain interface For ANSYS CFX based totally numerical answers, 3 methods are to be had to link rotating and stationary domains with each different. those are:

1. **Mixing-Plane technique**: It is a decrease order interface for RANS simulation, and it delivers average amounts on boundary of one area to the other and vice versa.

2. **Frozen-rotor method**:For RANS simulation, it is a better order interface. The real gliding data is obtained at the interface border, and the exact flow amounts are transported to the downstream domain at a specified rotating relative area role, and vice versa.

3. **Sliding mesh approach (temporary rotor-stator interplay)**:In this case, a higher order interface is used for the URANS CFD application than in the prior one. The relative position of spinning domain in actual physical time scales is taken into account, with the actual time float sections constantly passing to the downstream domain.

CHAPTER 4

RESULTS AND DISCUSSION

In this chapter,the computed data are represented as contours and graphs are plotted for visual understanding of the numerical solution.

4.1 CONTOURS

Tip Clearance=0.36mm.

In the Figure 8, the pressure contour for the tip clearance of 0.36mm is shown.The boundary conditions applied were Inlet Pressure=101 kPa and Outlet static Pressure=120 kPa.The maximum pressure obtained in the domain is 231 kPa and the minimum pressure is 48 kPa.

The maximum Pressure is obtained at flow separation point near the leading edge.

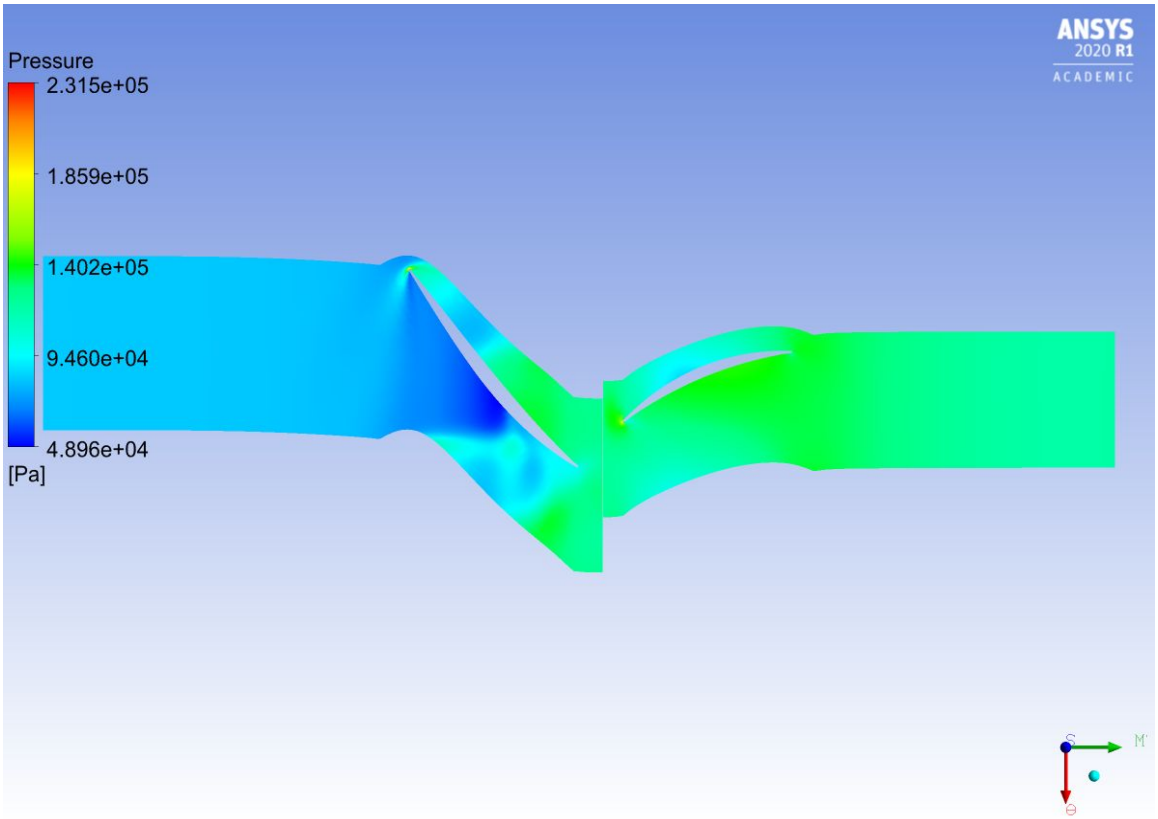

Figure 8: Pressure Distribution contour for the NASA Stage 37 with TC=0.36mm

In the Figure 9, the Velocity Distribution Field for the tip clearance of 0.36mm is shown.The boundary conditions applied were Inlet Pressure=101 kPa and Outlet static Presure=120 kPa.The maximum velocity obtained in the domain is 533 m/s and minimum velocity is 0 m/s.

Maximum velocity is obtained at the suction surface of rotor 37 blade.

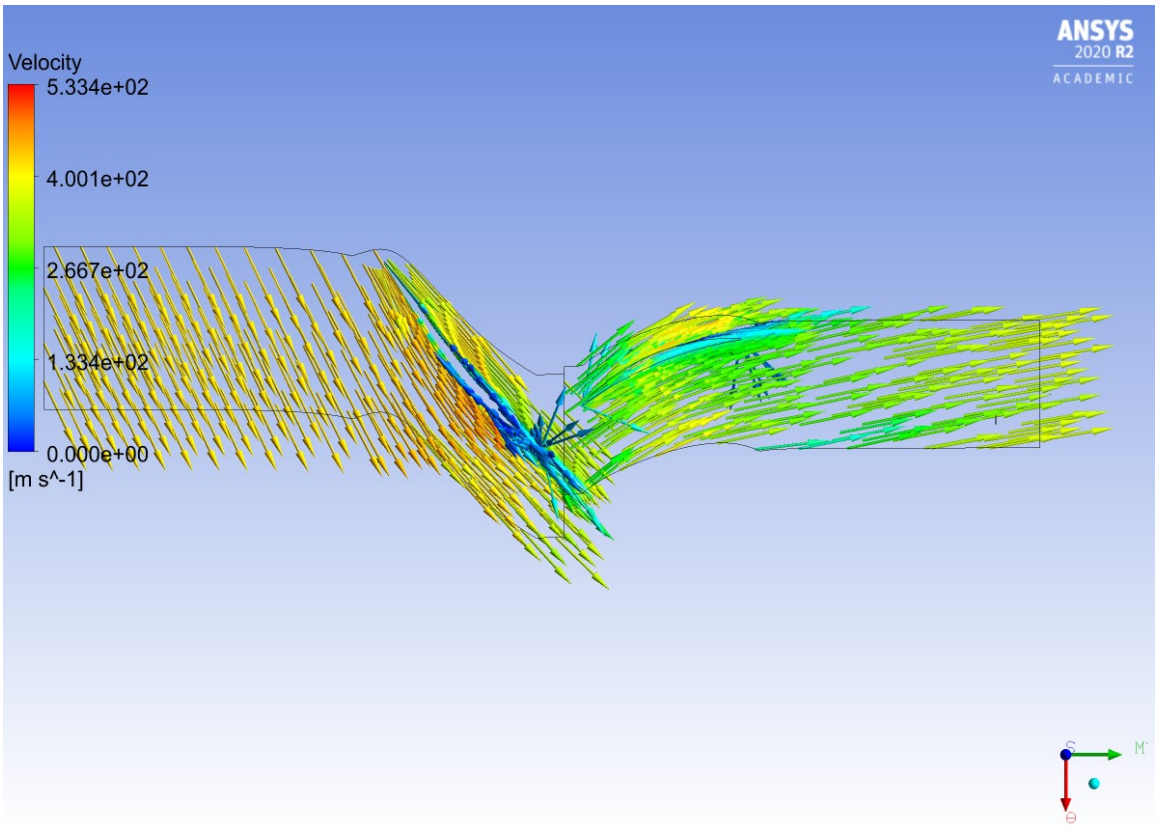

Figure 9: Velocity Distribution Field for the NASAStage 37 with TC=0.36mm

4.2 GRID INDEPENDENCE STUDY FOR TIP CLEARANCE OF 0.5 MM

In order to assess the influence of grid size on anticipated results, a grid independence study was performed. Numerical simulations with various grid densities were conducted at the compressor level. A rudimentary grid of about 0.3 million cells was created at first. The grid independence was then put to the test by building two bigger grids, each with around 0.4 million and 0.6 million cells. Performance characteristics of the compressor stage were determined for the three grid densities at 100 percent design speed in terms of variation of total pressure ratio and isentropic efficiency with variable mass flow rate, and these are displayed in Figures 10 and 11, respectively.

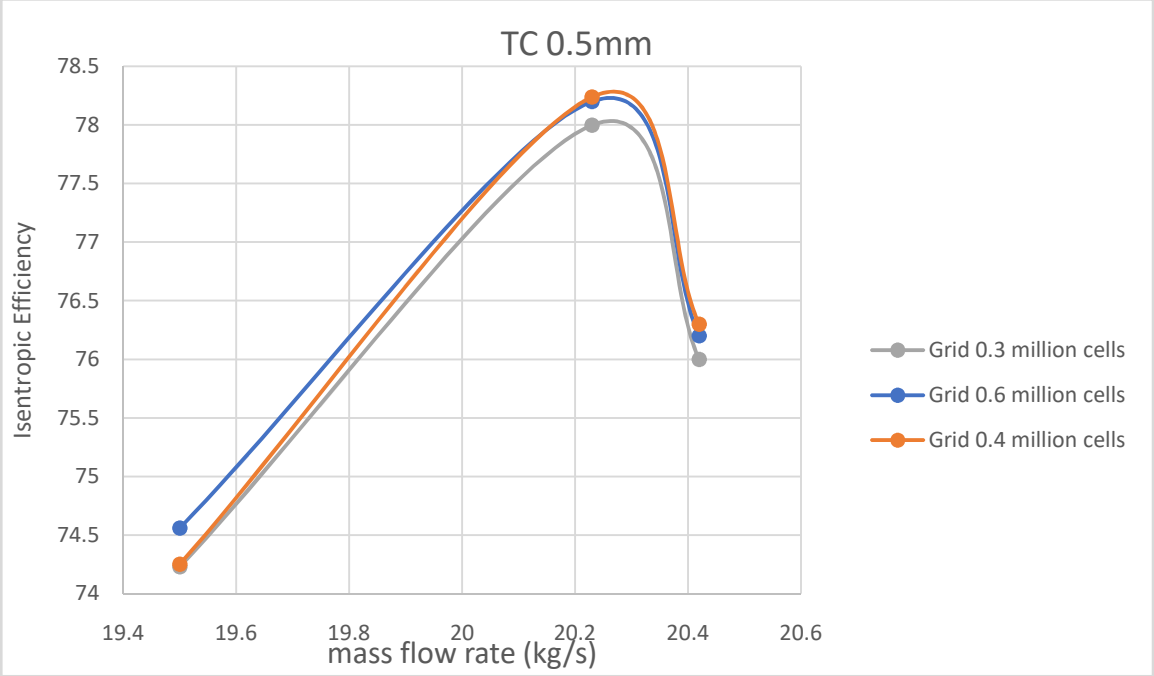

Figure 10: Isentropic Efficiency for the NASA Stage 37 with different grid sizes

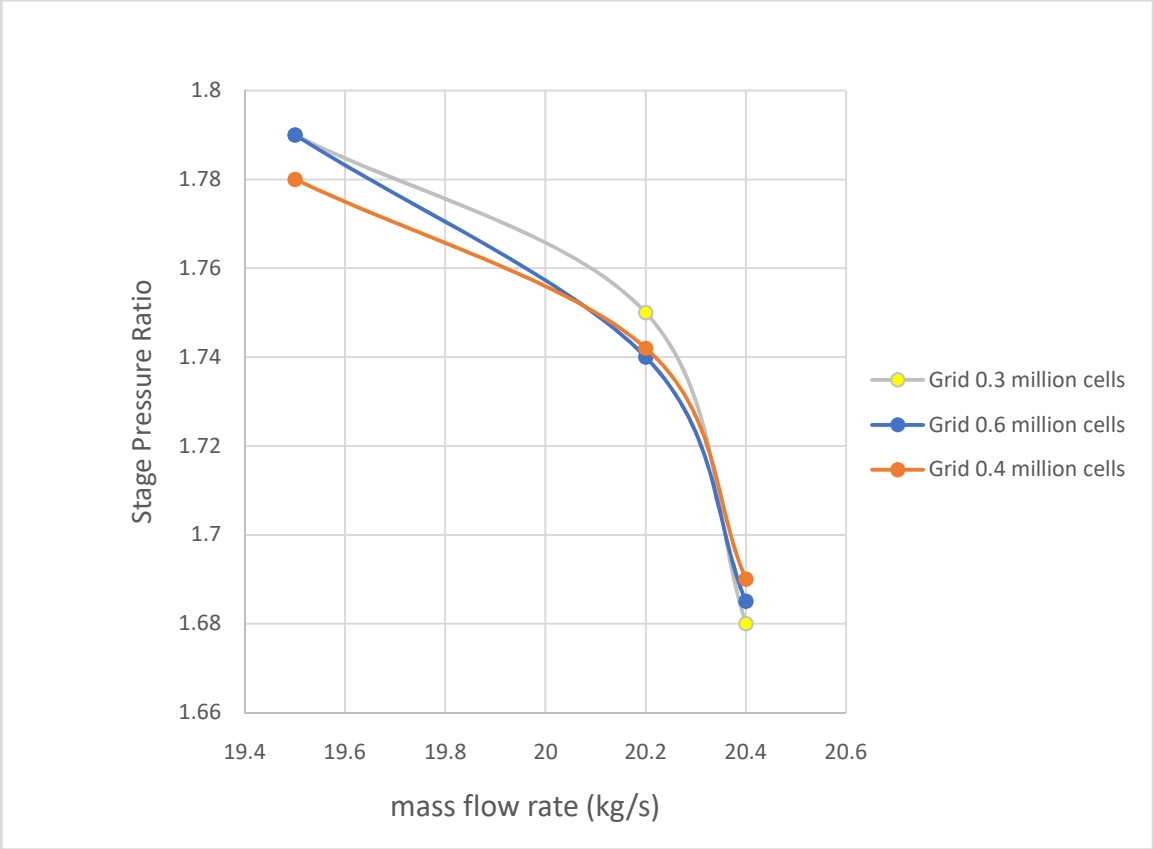

Figure 11: Stage Pressure Ratio for the NASA Stage 37 with different grid sizes

For all the three grids, the stage total pressure ratio and isentropic efficiency are under-predicted with respect to experimental data.

The findings of the grids with 0.3 and 0.4 million cells nearly coincide with each other, as can be seen in these graphs. The grid with about 0.6 million hexahedral components was chosen as the final mesh for additional calculations based on the grid independence analysis.

Tip clearance=0.5 mm

In the Figure 12, the pressure contour for the tip clearance of 0.5mm is shown.The boundary conditions applied were Inlet Pressure=101 kPa and Outlet static Presure=120 kPa.The maximum pressure obtained in the domain is 217 kPa and the minimum pressure is 46 kPa.

The maximum Pressure is obtained at flow separation point near the leading edge.

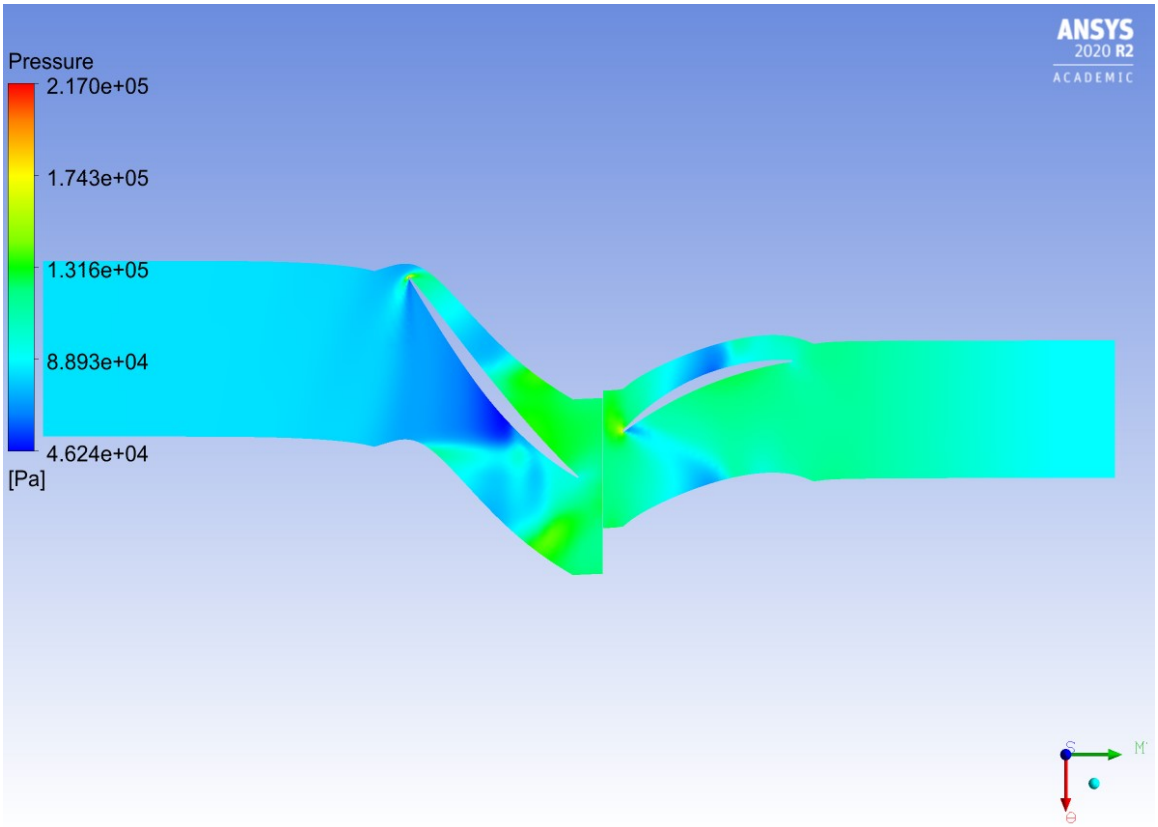

Figure 12: Pressure Distribution contour for the NASA Stage 37 with TC=0.5mm

In the Figure 13, the Velocity Distribution Field for the tip clearance of 0.5mm is shown.The boundary conditions applied were Inlet Pressure=101 kPa and Outlet static Presure=120 kPa.The maximum velocity obtained in the domain is 532 m/s and the minimum velocity is 0 m/s.

The maximum velocity is obtained at the suction surface of the rotor 37 blade.

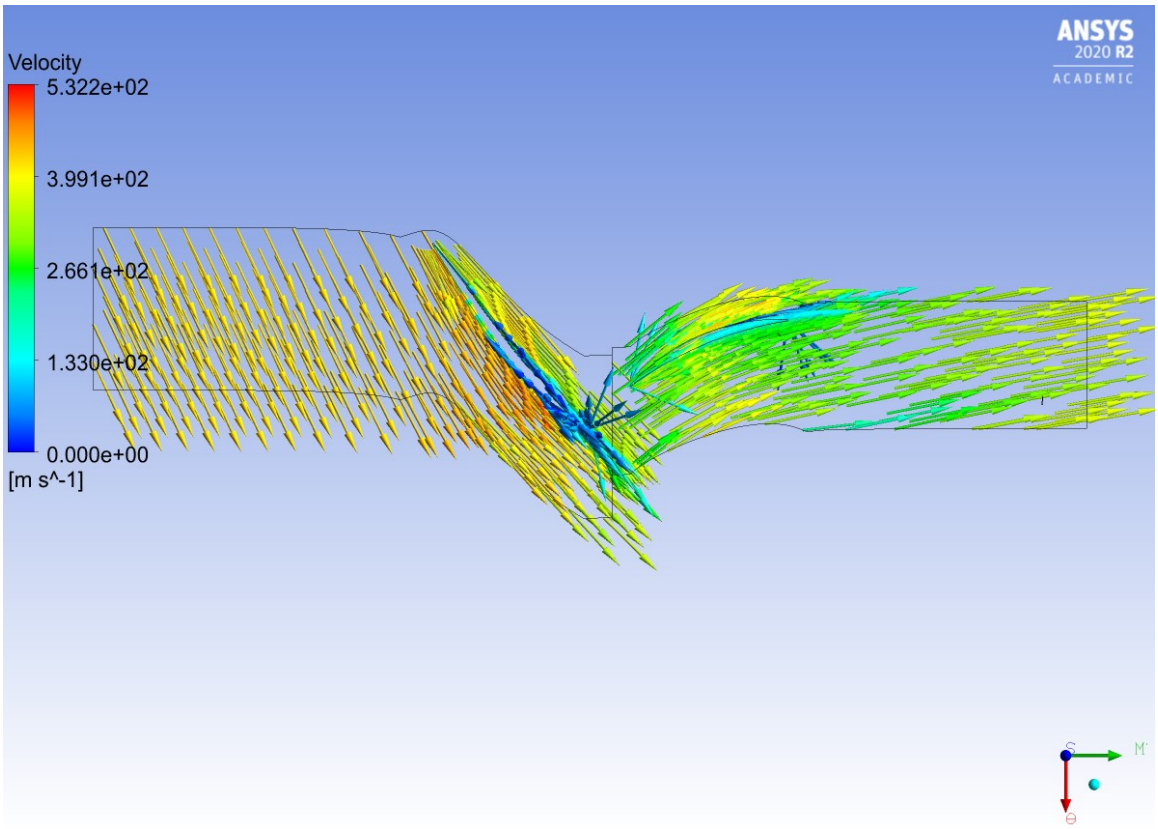

Figure 13: Velocity Distribution Field for the NASA Stage 37 with TC=0.5mm

In the Figure 14, the variation of stage pressure ratio is plotted against the variable mass flow rate for the tip clearance of 0.5 mm.It can be observed that the stage pressure ratio increases with decrease in the mass flow rate.

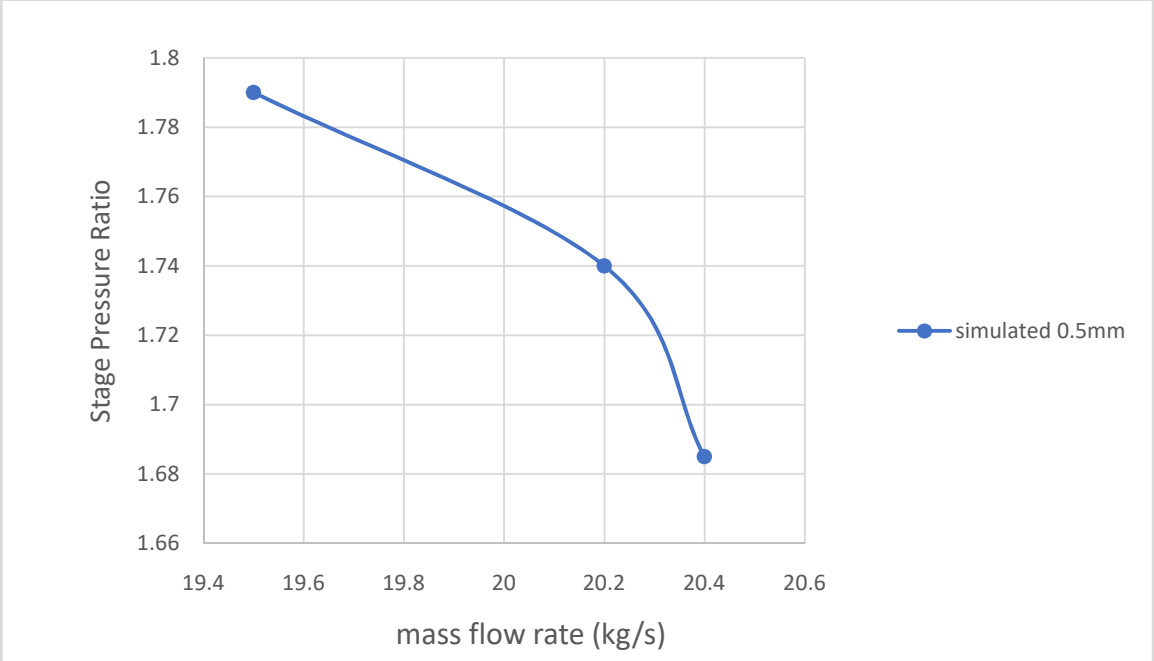

Figure 14: Computed stage pressure ratio for the NASA Stage 37 with TC 0.5 mm

In the Figure 15, the variation of Isentropic Efficiency is plotted against the variable mass flow rate for the tip clearance of 0.5 mm. It can be observed that the Isentropic Efficiency increases with increase in the mass flow rate reaches a maximum value and then gradually starts decreasing.

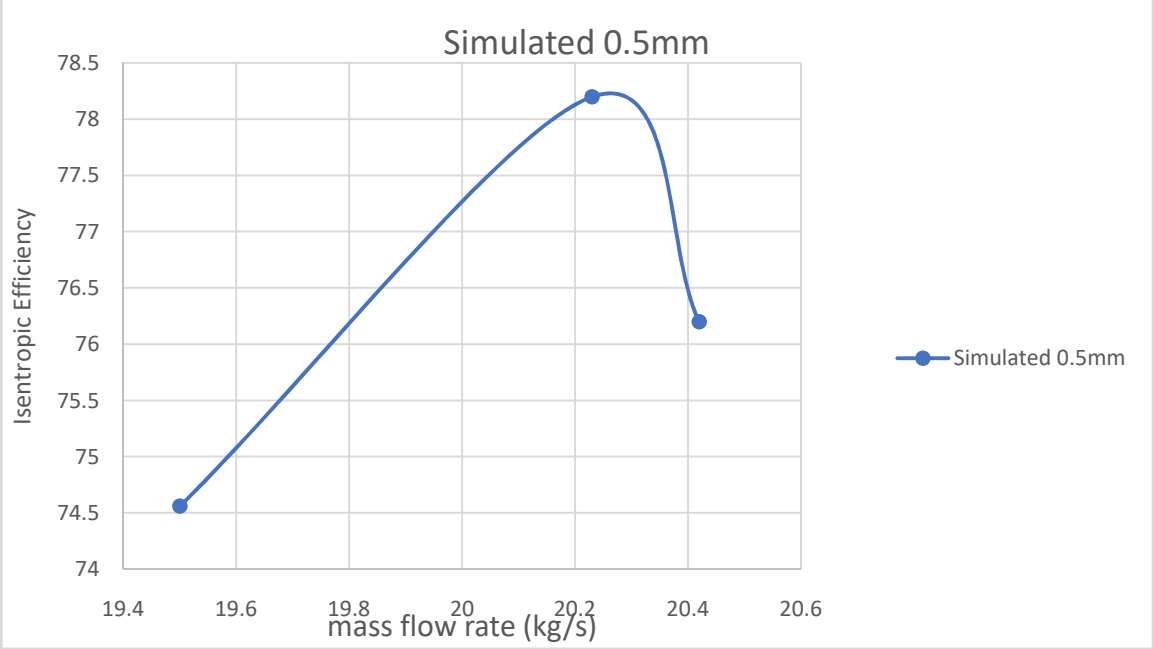

Figure 15: Computed Isentropic Efficiency for the NASA Stage 37 with TC=0.5 mm

CHAPTER 5

VALIDATION

In this chapter,the computed results are compared with experimental data for validation purposes.The percentage of error is calculated with the help of graphs presented below.

In the Figure 16,the experimental data from the research paper is plotted for stage pressure ratio and mass flow rate.It is compared with the computed data obtained for tip clearance of 0.36mm which is the design parameter.

The average percentage of error obtained between experimental and the computed data is around 7.2% for mass flow rate of 20.2 kg/s.

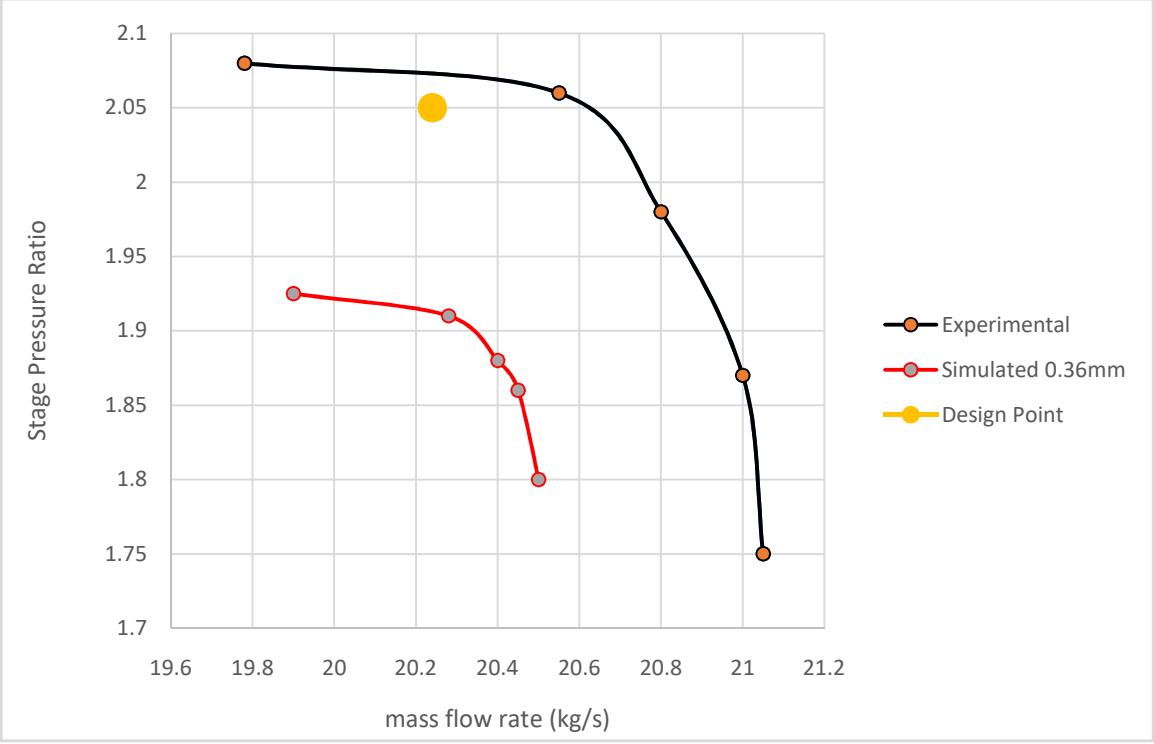

Figure 16:Comparison of stage Pressure RatioSimulated data with the experimental data for 0.36mmfor the NASA Stage 37

In the Figure 17, the experimental data from the research paper is plotted for Isentropic Efficiency and mass flow rate. It is compared with the computed data obtained for tip clearance of 0.36 mm which is the design parameter.

The error obtained between the experimental and the computed data is different for variable mass flow rate.

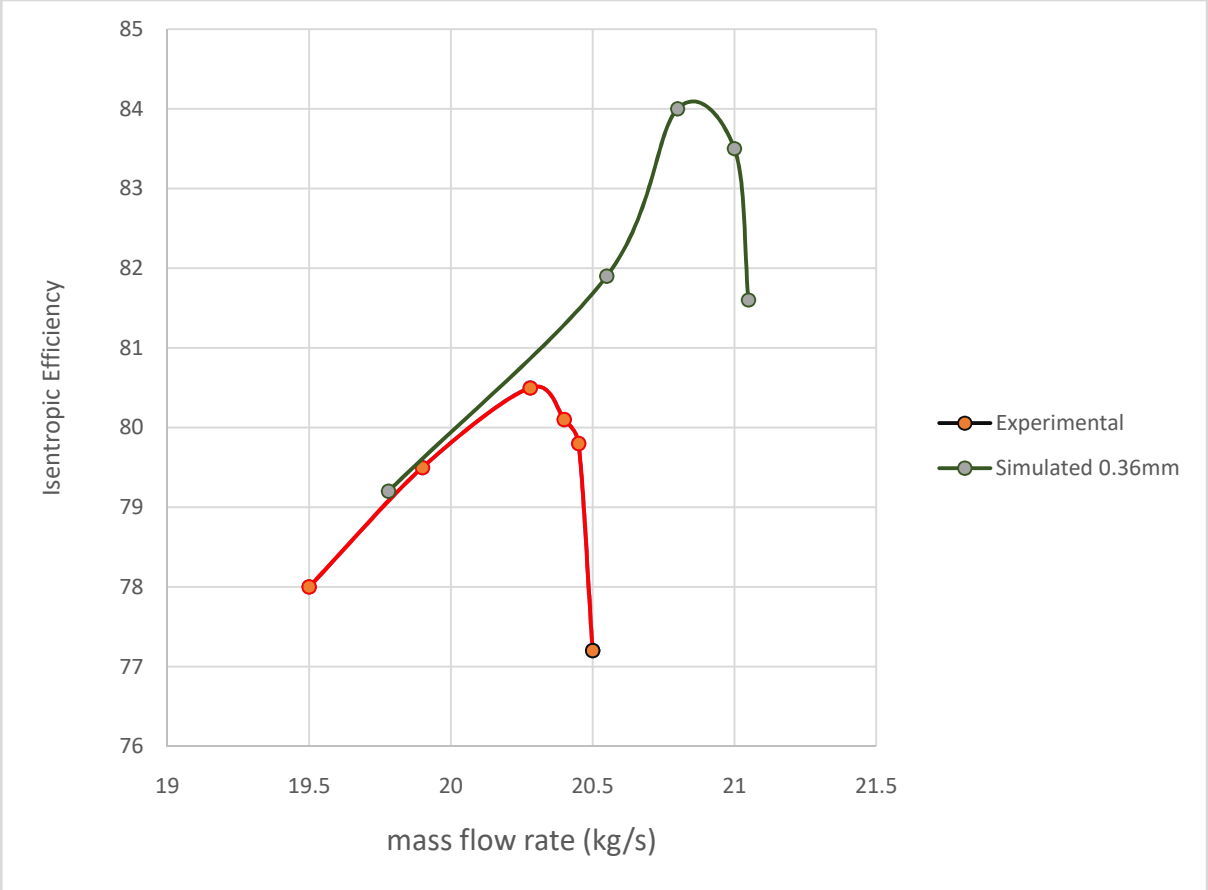

Figure 17: Comparison of Isentropic Efficiency simulated data with the experimental data for 0.36mm for the NASA Stage 37

In the Figure 18, the computed data of stage pressure ratio for the design tip clearance of 0.36 mm is compared with computed data obtained for tip clearance of 0.5 mm. which is the design parameter.

The average percentage of difference obtained between both the computed data is around 6.91% for mass flow rate of 20.2 kg/s.

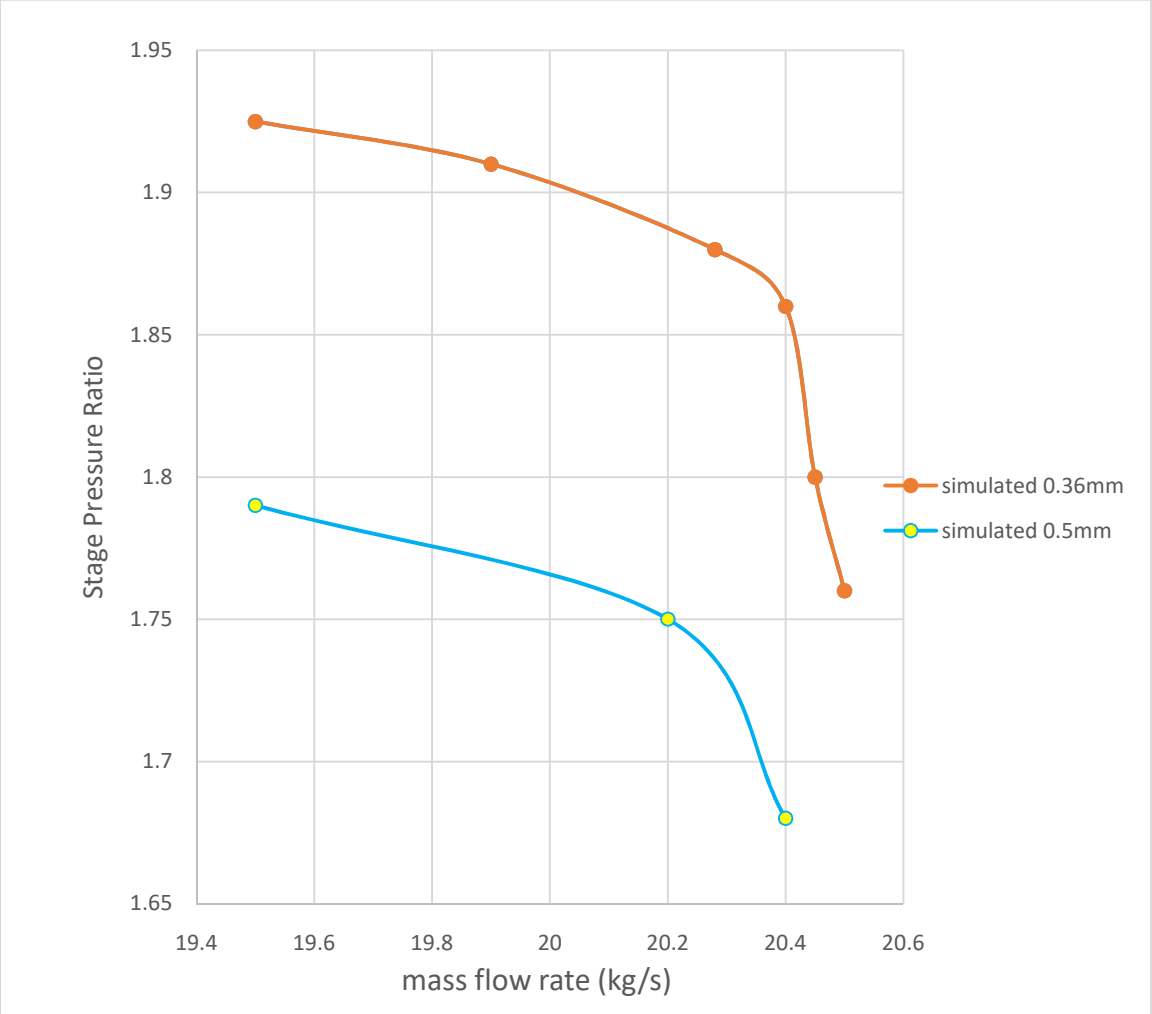

Figure 18: Comparison of computed data for Tip clearance 0.5mm with 0.36mm for Stage Pressure Ratio

In the Figure 19, the computed data of Isoentropic Efficiency for the design tip clearance of 0.36 mm is compared with the computed data obtained for tip clearance of 0.5 mm. which is design parameter.

The average percentage of difference obtained between both the computed data is around 2.97% for mass flow rate of 20.2 kg/s.

.

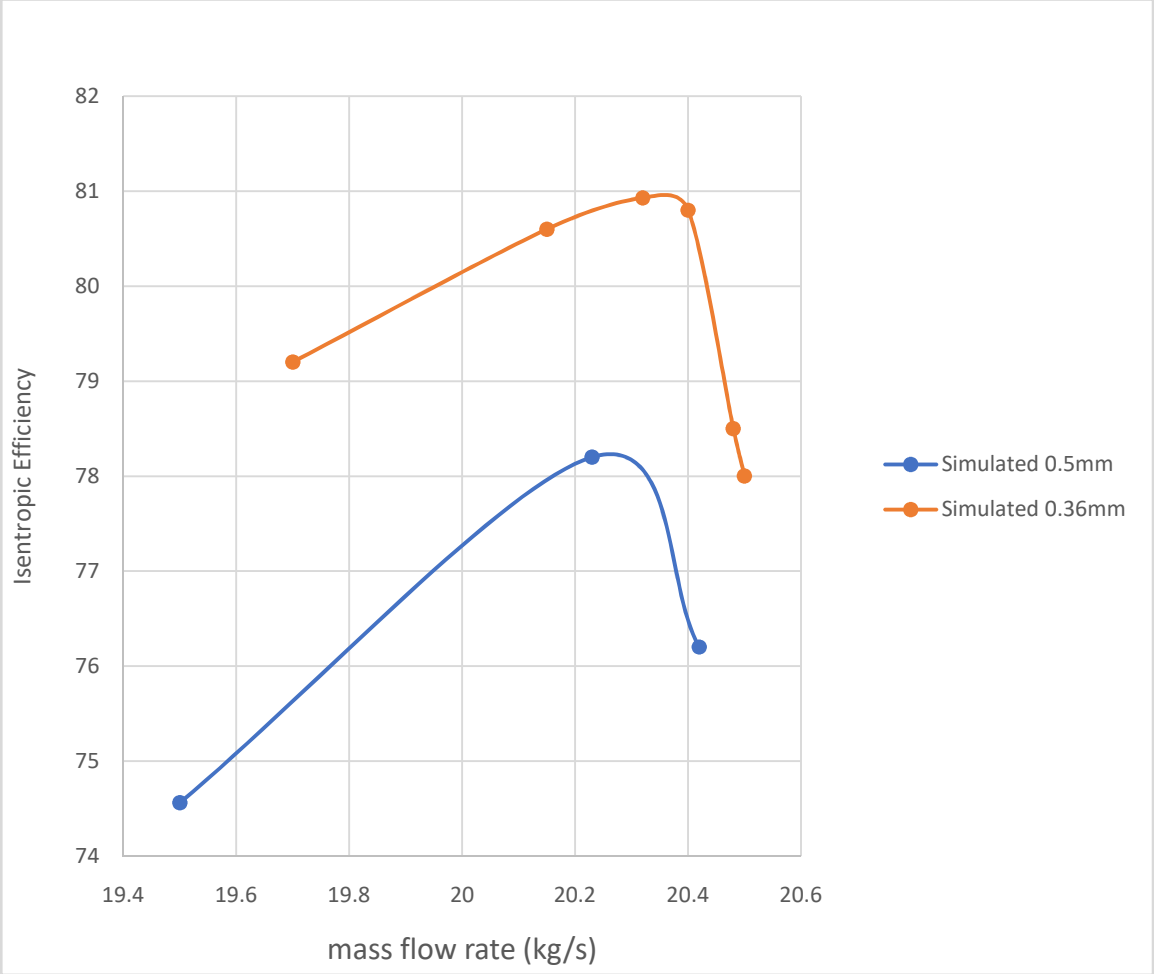

Figure 19:Comparison of computed data for Tip clearance 0.5mm with 0.36mm for Isentropic efficiency

CHAPTER 6

CONCLUSION

6.1 CONCLUSION

- Numerical research on the unmarried degree NASA37 transonic axial compressor with a rotor tip clearances of 0.5mm turned into carried out through numerical simulations at a 100% design rotational speed.
- To understand impact of tip clearance on performance of an axial compressor, previous experimental and computational research was undertaken.
- With these result we can understand that rotor tip the efficiency of axial compressor. The existing research is limited to a single stage transonic compressor with a low aspect ratio and a high pressure ratio.
- From the obtained results we can conclude that with increment in tip clearance stage pressure ratio decreases due to which isentropic efficiency also decreases.
- It is evident that with increase in mass flow rate stage pressure ratio increases.
- The Isentropic Efficiency first increases with increase in mass flow rate than reaches a maximum and then gradually starts decreasing.
- When compared to the TC 0.36mm simulated data with the TC 0.5mm Simulated data, therereduction of 6.91% in the Stage Pressure values at mass flow rate of 20.2kg/s.
- When compared to the TC 0.36mm simulated data with the TC 0.5mm Simulated data, there was reduction of 2.97% in the Isentropic Efficiency value at mass flow rate of 20.2kg/s.
- According to the findings of the current research, optimal rotor tip clearance enhances compressor overall performance by minimising losses due to tip leakage and secondary flow interaction.

6.2 SCOPE OF FUTURE WORK

The effect of tip clearance on NASA stage 37 is the focus of this research. Further research into the many impacts of tip clearance, such as secondary flows formed by a pressure gradient on blade's span and boundary scraping caused by tip clearance, can be done to gain a better knowledge of the consequences of tip clearance. For further advancement in this field, the combination of swirl and total-pressure distortion on turbomachinery can be studied.

This thesis focuses on the steady state analysis.It can be extended to transient analysis for future work.

REFERENCES

[1] Cameron, J. D. et al., "The Influence of Tip Clearance Momentum Flux on Stall Inception in a High-Speed Axial Compressor" ASME Journal of Turbo machinery, 2013, Vol.135.

[2] Copenhaver, W.W. et al, (1996) "The Effect of Tip Clearance on a Swept Transonic Compressor Rotor" ASME Journal of Turbomachinery, 1996, Vol.118.

[3] Furukawa, M., Inoue, M., Saiki, K. and Yamada, K., "The Role of Tip Leakage Vortex Breakdown in Compressor Rotor Aerodynamics", ASME Journal of Turbomachinery, 1999, Vol.121.

[4] Gerolymos, G. A. and Vallet, I., "Tip-clearance and secondary flows in a transonic compressor rotor", 1998, ASME Journal of Turbomachinery.

[5] Lakshminarayana B., Zaccaria, M. and Marathe, B., "The Structure of Tip Clearance Flow in Axial Flow Compressors", ASME Journal of Turbomachinery, 1995, Vol.117.

[6]M. Hoeger, M. et al., "Numerical Simulation of the ShockTip Leakage Vortex Interaction in a HPC Front Stage", 1999, ASME Journal of Turbo machinery Vol.121.

[7]P.V. Ramakrishna, M. Govardhan, Stall characteristics and tip clearance effects in forward swept axial compressor rotors, J. Therm. Sci. 18 (2009) 40–47.

[8] Ried, L. and Moore, E. M., "Design and Overall Performance of Four Highly Loaded, High Speed Inlet Stages for an Advanced High Pressure Ratio Core Compressor", NASA TP 1337, 1978.

[9] S.E. Gorrell, T.H. Okiishi, W.W. Copenhaver, Stator-rotor interactions in a transonic compressor – part 1: effect of blade-row spacing on performance, ASME J. Turbomach. 125 (2) (2003) 328–335.

[10] S.E. Gorrell, T.H. Okiishi, W.W. Copenhaver, Stator-rotor interactions in a transonic compressor – part 2: description of a loss-producing mechanism, ASME J. Turbomach. 125 (2003) 336–345.

[11] S. Sakulkaew, C.S. Tan, E. Donahoo, C. Cornelius, M. Montgomery, Compressor efficiency variation with rotor tip gap from vanishing to large clearance, J. Turbomach. 135 (2013) 35–48.

[12] S. Yoon, R. Selmeier, P. Cargill, P. Wood, Effect of the stator hub configuration and stage design parameters on aerodynamic loss in axial compressors, J. Turbomach. 137 (2015) 091001.

[13] Subbaramu S., Q.H. Nagpurwala , Mahesh K. Varpe and H.K. Narahari Effect of Tip Leakage and Secondary Flow Interaction on the Performance and Stability of a Transonic Axial Compressor Stage.Proceedings of the Asian Congress on Gas Turbines ACGT2016 14-16 November 2016.

[14]Sriram, A. T. and Manjunath, D. C. (2016) Numerical Study of Pre-Diffuser Performance with Axial Flow Compressor, Proceedings of Asian Congress on Gas Turbines, 14-16 November 2016.

[15] Storer J.A. and Cumpsty N.A., "Tip Leakage Flow in Axial Compressors", ASME Journal of Turbomachinery, 1991, Vol.113.

[16] Suder, K.L. and Celestina, M.L., "Experimental and Computational Investigation of the Tip Clearance Flow in a Transonic Compressor Rotor", NASA TM-106711, 1994.

[17]Syed Noman Danish, Shafiq Rehman Qureshi, Malik Muhammad Imran, Salah Ud-Din Khan, Muhammad Mansoor Sarfraz, et al.. Effect of tip clearance and rotor–stator axial gap on the efficiency of a multistage compressor. Applied Thermal Engineering, Elsevier, 2016, 99, pp.988-995. ff10.1016/j.applthermaleng.2016.01.132ff. ffhal-01574153f.

[18] Thompson, D.W. et al, "Experimental Investigation of Stepped Tip Gap Effects on the Performance of a Transonic Axial Flow Compressor Rotor" ASME Journal of Turbomachinery, 1998, Vol.120.

[19] X. Deng, H. Zhang, J. Chen, Unsteady tip clearance flow in a low speed axial compressor rotor with upstream and downstream stators, in: ASME Turbo Expo 2005: Power for Land, Sea, and Air, Nevada, USA, Jun 6–9, 2005.

[20] Y. Tang, C. Hung, Y. Chang, Performance improvements in low side scroll compressor with extended operation speeds, Appl. Therm. Eng. 31 (2011) 3542–3551.

[21] Yamada, K., Funazaki, K. and Furukawa, M., "The Behavior of Tip Clearance Flow at Near Stall Condition in a Transonic Axial Compressor Rotor", ASME Turbo Expo, 2007, Montreal, Canada.